Charge Persistence in InGaAs/InP Single-Photon Avalanche Diodes

Niccolò Calandri, *Student Member, IEEE*, Mirko Sanzaro, *Student Member, IEEE,* Alberto Tosi, *Member, IEEE,* Franco Zappa, *Senior Member, IEEE,*

***Abstract* — We present a detailed characterization and modeling of the charge persistence effect that impacts InGaAs/InP Single-Photon Avalanche Diodes (SPADs). Such phenomenon is due to holes that pile-up at the heterointerface outside the active area and has two main consequences: i) higher noise (equivalent to higher dark count rate), not decreasing as expected at low temperature; and ii) possible distortion of the acquired time-resolved waveforms (due to such signal-correlated noise). We propose a model that describes: i) the generation of holes at the detector periphery in the InGaAs layer; ii) their accumulation at the heterointerface; iii) their subsequent diffusion towards the active area within the InGaAs layer; iv) their resulting drift to the high field depleted InP region, where the unwelcome spurious avalanche is eventually triggered. We support our model by detailed experimental measurements and simulations. Finally, we propose simple approaches for designing detectors less sensitive to this type of noise.**

***Index Terms* — Photodetectors, Single-Photon Avalanche Diode, SPAD, hetero-barrier, charge trapping, photon counting, near-infrared detector, Avalanche Photodiode, APD.**

I. Introduction

Near-Infrared single-photon detectors enable a growing number of applications, e.g. 3D laser ranging (LIDAR), quantum cryptography, optical VLSI circuit testing, time-resolved spectroscopy, which require to detect very faint optical signals (down to the single-photon level) with very good time accuracy (better than 100 ps). Compared to other detectors, Single-Photon Avalanche Diodes (SPADs) have the distinctive advantages of solid-state devices (small size, low bias, low power consumption, high reliability) and offer high detection efficiency, excellent time precision, and easy and reliable practical implementation [1]. Indeed, in the last years, significant progress has been made in design and material quality of InGaAs/InP SPADs, leading to dark count rates (DCR) as low as few kcps (counts per seconds) at 230 K, with photon detection efficiency (PDE) higher than 20%, and timing jitter lower than 100 ps [2][3].

Primary dark counts (due to thermal generation and trap-assisted tunneling) and afterpulsing are the main noise sources in InGaAs/InP SPADs. However, an additional contribution, which is often overlooked, is due to holes that are generated within the neutral region of the undoped InGaAs layer and that diffuse towards the active area. Such carriers may exhibit lifetimes in the microseconds range and hundreds of µm diffusion lengths [4][5]. Consequently, when the InGaAs/InP SPAD is operated in the usual gated mode, these carriers can accumulate during the OFF time interval (when the electric field is low) and then trigger delayed avalanches during the next ON time interval (when the electric field is high). As a result, some holes generated within few diffusion lengths from the active area's depleted region can trigger spurious avalanches that increase the noise. Moreover, since lifetime increases at lower temperature, such hole accumulation gets higher when cooling the detector, thus impairing the lowest achievable DCR (see Section III-D).

Minority carrier diffusion from neutral regions to the depleted region is a known issue for both PIN photodiodes and APDs (Avalanche Photodiodes), where unwelcome slow diffusion tails limit their bandwidth [6]. However, in such devices its impact on dark current is negligible because surface leakage and tunneling currents dominate [7]. Instead, for SPADs, dark counts are dominated by bulk generation mechanisms and, therefore, such carriers diffusing from the neutral peripheral regions towards the central depleted region can have an important impact.

Beside thermal generation, in neutral regions carriers can be generated by photons absorbed outside the active area. Even though many applications rely on optical fiber light coupling, which focuses most of the photons into the active area, there are many applications where free-space coupling is the only viable approach, thus being prone to the absorption of photons outside the nominal active area. A few examples are: i) time-resolved diffuse optical tomography, where a very large numerical aperture device is highly desirable in order to maximize the collection efficiency [8][9] ii) biomedical applications, where the efficiency of light collection could be increased considerably by using a larger-diameter fiber with high numerical aperture, thus requiring a free-space coupled detector [8][9]; iii) InGaAs/InP SPADs arrays, where, even when microlenses are employed, light hits also neutral regions among pixels active areas [10].

The authors are with the Dipartimento di Elettronica, Informazione e Bioingegneria, Politecnico di Milano, Milano 20133, Italy (e-mail: niccolo.calandri@polimi.it; mirko.sanzaro@polimi.it; alberto.tosi@polimi.it; franco.zappa@polimi.it).

Moreover, in some of these applications time-gating is required in order to gate-off a strong unwelcome signal (e.g. a strong laser back-reflection) arriving few hundreds of picoseconds before the faint signal to be measured. In fact, recently a few authors found a correlation between a strong light pulse before gating the detector ON and the DCR increase [11][12][13]. Ref. [12] and [13] show that light absorbed during OFF time interval affects photon counting optical time-domain reflectometry (OTDR) and authors explained those phenomena as carrier trapping and release within the multiplication region (as for afterpulsing), enhanced by the finite multiplication gain during gate-off.

In this paper, we describe the experimental characterization and the derived model for this "charge persistence" effect. We outline the major impacts on detector operation and, with the support of simulations, we propose practical design hints for minimizing this noise contribution.

Section II introduces the structure of the InGaAs/InP SPADs under investigation. Section III reports the main results of our experimental characterization. Section IV details the proposed physical model and its validation with experimental data. Eventually, Section V draws conclusions.

II. Device structure

The InGaAs/InP SPADs under investigation have the Separate Absorption, Graded, Charge, and Multiplication (SAGCM) structure shown in Fig. 1. We will refer to samples from Ref. [1] as PLI SPADs (with back-side illumination), while those from Ref. [3] as PoliMi SPADs (with front-side illumination). A near-infrared photon absorbed in the InGaAs absorption layer ($E_g \sim 0.75$ eV) creates a photogenerated hole, which drifts towards the high field region where it can trigger the impact ionization process within the InP multiplication layer ($E_g \sim 1.35$ eV), thus giving rise to a self-sustaining avalanche multiplication process. Between absorption and multiplication regions, a charge layer shapes the electric field profile in order to keep high electric field only within the InP multiplication layer, while lowering it within the absorption InGaAs layer for limiting tunneling and field-assisted thermal carrier generation in that low band-gap layer. Additionally, an InGaAsP graded layer is designed to avoid holes pile-up at the heterointerface, which would degrade photogenerated holes transit time and would impair the detector timing response.

The high electric field is confined within the active area by means of double p-type Zn diffusions: in order to minimize premature edge breakdown, a shallow diffusion with wide diameter (39 µm, compared to the 25 µm of the active area for PoliMi SPADs) reduces electric field peaking at the active area's edge.

Fig. 1: Schematic cross-section of an InGaAs/InP SPAD with SAGCM heterostructure. The InGaAs absorption layer has been divided into three regions: high field, low field and neutral regions. PoliMi SPADs have $x_1 = 25$ µm and $x_2 = 7$ µm.

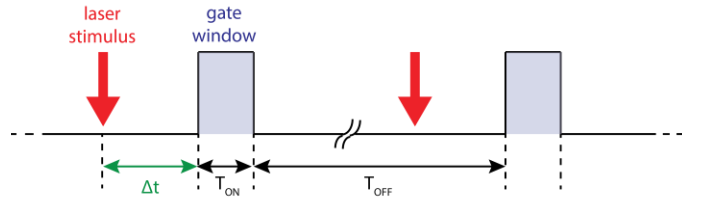

Fig. 2: Illumination scheme: the laser pulse arrives in advance (Δt) with respect to the gate-on window. No photon arrives during the gate window and the device is flood illuminated, except where otherwise stated.

III. Experimental Characterization

For the experimental measurements, we employed both PoliMi SPADs and PLI SPADs, since charge persistence is common to many available InGaAs/InP SPAD detectors. In the following characterization, the devices are operated in gated mode, with an OFF time longer than 100 µs in order to have negligible afterpulsing noise, as reported in [1] for PLI devices and in [3] for PoliMi ones (see also Fig. 8 in section III.D).

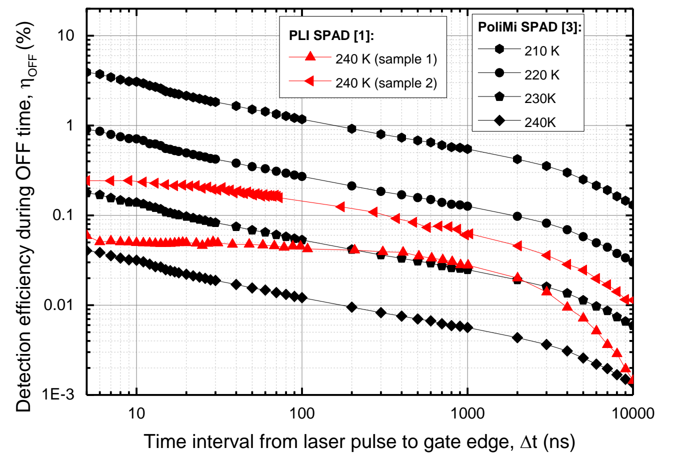

Fig. 3: Dependence of the measured detection efficiency on the time interval Δt between the laser pulse to the gate-on leading edge: these avalanches are triggered by photons absorbed when the SPAD is OFF, i.e. biased below the breakdown level, and whose photogenerated hole reaches the multiplication region during a successive ON-time. The devices are flood illuminated and photons are absorbed also in their periphery. Operating conditions: $V_{EX} = 5$ V, $V_{UV} = 0.5$ V, $T_{ON} = 20$ ns, $T_{OFF} = 100$ µs.

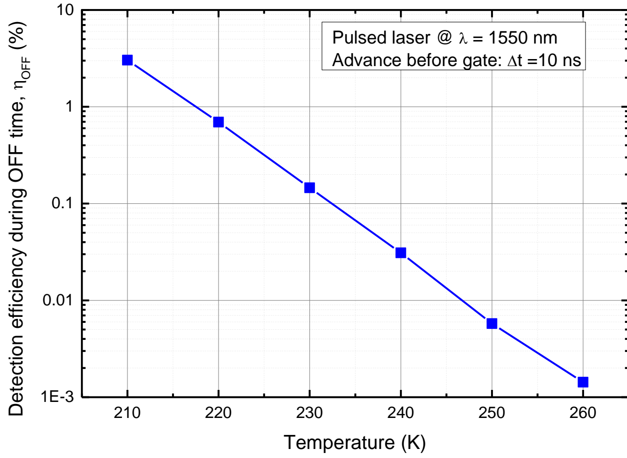

Fig. 4: Temperature dependence of the detection efficiency during OFF time for a PoliMi InGaAs/InP SPAD. Operating conditions: $V_{EX} = 5$ V, $V_{UV} = 0.5$ V, $T_{ON} = 20$ ns, $T_{OFF} = 100$ µs.

A. *Detection efficiency during OFF time*

With the illumination scheme shown in Fig. 2, we measured the SPAD sensitivity to photons reaching the detector during the OFF-time and its dependence on the time separation Δt between the laser pulse and the gate leading edge. We employed a pulsed laser at 1550 nm and a power density of few nanowatts/mm^2. At this wavelength, photons can be absorbed only in the InGaAs layer and, given the very narrow (20 ps) pulse width, photogeneration of carriers is well confined in time. Devices under test were flood illuminated (i.e. both the active area and the peripheral regions are uniformly illuminated). As demonstrated in Sec. III.C, flood illumination is indeed a critical condition for charge persistence.

We define the detection efficiency during OFF time as:

$$ {}_{OFF}\,(\Delta t) = \frac{CR_{OFF}(\Delta t)}{n_{ph}} = {}_{ON} \cdot \frac{CR_{OFF}\,(\Delta t)}{CR_{ON}} $$

$CR_{OFF}(\Delta t)$ is the net count rate (i.e. after DCR subtraction) measured in the ON-time for a laser pulse reaching the device during the OFF-time at a time Δt before the gate. n_{ph} is the flux of photons reaching the detector during the laser pulse, which has been estimated as $n_{ph} = CR_{ON}/\eta_{ON}$, where CR_{ON} is the net count rate when the same laser reaches the device during the ON-time and η_{ON} is the standard detection efficiency of the SPAD during gate-on.

Fig. 3 compares $\eta_{OFF}(\Delta t)$ of the two InGaAs/InP SPADs under investigation. At 240 K PLI SPADs show higher OFF detection efficiency than Polimi SPADs at short Δt delays. For $\Delta t > 1$ µs, $\eta_{OFF}(\Delta t)$ decreases abruptly for PLI SPADs. PoliMi SPADs instead exhibit a decay of η_{OFF} slower than PLI SPADs. Therefore, charge persistence effects may be affected by the device structure (cross-section, doping levels, thicknesses, etc.). Moreover, the exact impact of the charge persistence may vary from sample to sample (see the two samples of PLI SPADs in Fig. 3).

Fig. 4 show the temperature dependence of η_{OFF} for PoliMi SPADs at a given Δt value (10 ns): η_{OFF} exponentially increases by decreasing the operating temperature, eventually becoming the dominant noise contribution at low temperature and limiting the minimum operating temperature (see Fig. 7 in Sect. III.D). Moreover, as an example of the impact of this phenomena, in the scenario of time-resolved diffuse optical spectroscopy [8], with a signal of 0.01 photons per pulse and considering a PoliMi SPAD at 210 K, with $T_{ON} = 50$ ns, $V_{EX} = 5$V, a gate repetition rate of 10 kHz and the laser pulse absorbed 10 ns before each gate ON, the dark count rate increases by ~ 200%, from 3 kcps up to 9 kcps.

B. *Avalanche distribution during gate-on*

Using the illumination scheme of Fig. 2, we employed a Time-Correlated Single-Photon Counting (TCSPC) setup to acquire the time distribution of the charge persistence counts during gate-ON. Fig. 5 shows that at the beginning of the gate-ON there is a peak of spurious counts. Then, the counts distribution decays exponentially, with two time constants: a faster one (in the nanosecond range) due to holes drift from the close periphery (from region 2 to region 1 referring to Fig. 1), and a longer one (hundreds of nanoseconds), from the diffusion in the overall external region.

The 3 curves of Fig. 5 also show the temperature dependence of the spurious counts distribution after DCR subtraction. The time constant of the initial fast exponential decay slightly changes from 4.7 ns at 210 K down to 2.6 ns at 230 K. The slower one instead is almost constant (its time constant is about 100 ns). Moreover, the peak amplitude increases at lower temperatures.

C. *Dependence on photon absorption position*

With the illumination scheme of Fig. 2, we also measured the spatial distribution of the phenomenon by introducing a

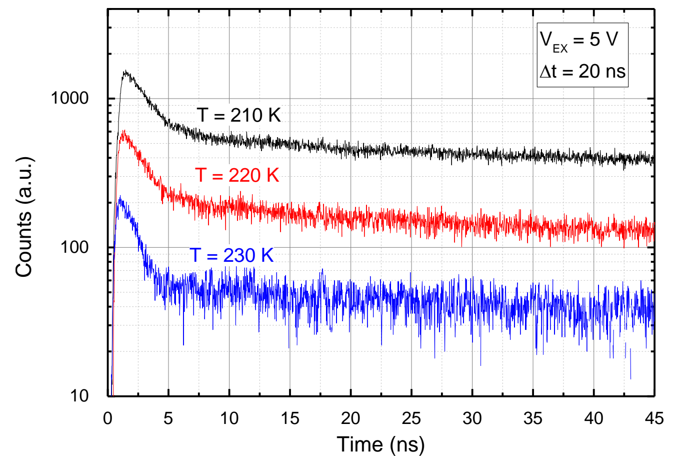

Fig. 5: Time distribution during gate-ON of the spurious counts due to photons absorbed before the gate-ON at Δt = 20 ns at different temperatures. All measurements have the same acquisition time and DCR is subtracted. Operating conditions: $V_{EX} = 5$ V, $V_{UV} = 0.5$ V, $T_{ON} = 50$ ns, $T_{OFF} = 100$ µs, Temperature = 225 K.

focusing optics that creates a 5 µm diameter spot from the 1550 nm pulsed laser. The device active area and its periphery have been scanned with 2 µm steps and the count rate has been acquired for each spot position. The resulting 2D plot, reported in Fig. 6, is a map of the origins of the spurious counts. As shown in Fig. 6, photons that most effectively enhance the count rate are only those absorbed outside the device active area (delimited by the solid line in Fig. 6) and even outside the shallow diffusion (see the dashed line). This implies that photogenerated carriers move through the InGaAs layer from the accumulation point to the active area, where they trigger an avalanche during the subsequent gate-on window.

As can be observed by comparing the two plots in Fig. 6, the higher the time elapsed from the laser stimulus to the gate-ON window, the greater the area in which photo-generation can enhance the count rate. From Δt = 10 ns to Δt = 100 ns, the extension of the persistence area (i.e. the torus thickness) increases from 20 µm to 35 µm.

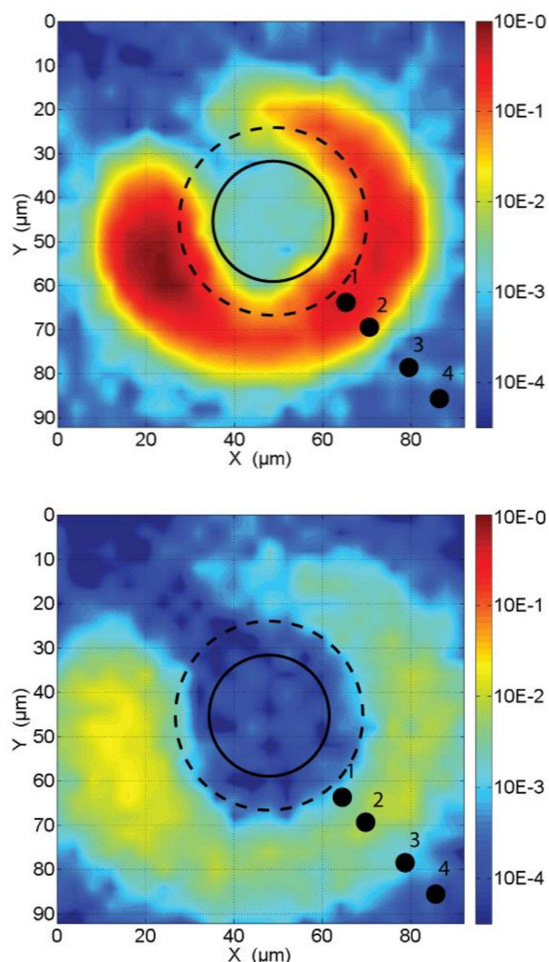

Fig. 6: Normalized maps of spurious counts when scanning the SPAD active area and its periphery with a pulsed laser stimulus before the gate with Δt = 10 ns (top) and Δt = 100 ns (bottom), respectively. The active area is delimited by a solid line and the edge of the shallow diffusion by the dashed line. The anode metal stripe shields the laser illumination in the top left corner of the figure. Points 1 to 4 are the four spot positions mentioned in legend of Fig. 12 and where the curves therein reported are acquired. Operating conditions: V_{EX} = 5 V, V_{UV} = 0.5 V, T_{ON} = 20 ns, T_{OFF} = 100 µs, Temperature = 225 K.

This measurement is in contrast with an afterpulse-like physical interpretation of the phenomenon as reported in previous works [12][13], because trapping of avalanche carriers by deep levels would highlight the active area and not its periphery. From our measurements, instead, we infer that the charge persistence effect is mainly due to holes not able to cross the heterobarrier that then diffuse from the neutral regions to the active area. The result is that even the area outside the active area is sensitive to photons, since absorbed photon can give additional delayed counts.

D. *Persistence counts increase DCR*

DCR of three different devices are plotted as function of temperature in Fig. 7. Considering PoliMi SPAD sample 1, the one used for the charge persistence measurements, the dark count rate at 275 K is ~ 400 kcps. By cooling the SPAD down to 225 K, DCR is strongly reduced by about two orders of magnitude, indicating that DCR is dominated by thermal generation in the active area. Below 225 K, the slope of this curve drastically reduces, while from 220 K to 175 K DCR even increases. Concerning the latter temperature, by decreasing the temperature the electric field at breakdown decreases because of reduced carrier scattering. Therefore, during the OFF time the lower electric field leads to a reduction of the mean rate to cross the heterobarrier. As a result, more holes, coming from the periphery to the active area, accumulate at the heterobarrier during the OFF time period and, eventually, trigger avalanches during the subsequent ON time period. We can exclude a significant contribution from afterpulsing given the sufficiently long OFF time we set (100 µs), as shown in Fig. 8: at 175 K, the dark count rate with T_{OFF} = 100 µs is comparable to that with much longer T_{OFF}.

Considering the other two devices (PoliMi SPAD sample 2 and PLI SPAD sample 1), the dark count rate dependence on temperature is monotonic: there is negligible charge persistence effect on the dark counts because the electric field at the edge of the active area is higher. Indeed, if we consider PoliMi SPADs, sample 2 was designed to have higher electric field under the shallow region compared to sample 1, thus

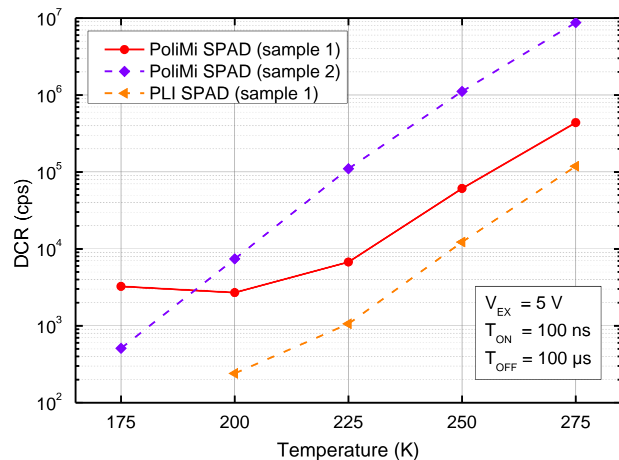

Fig. 7: Dark count rate versus temperature for three different InGaAs/InP SPADs. The OFF time was keep longer than 100 µs in order to avoid keep afterpulsing effect low.

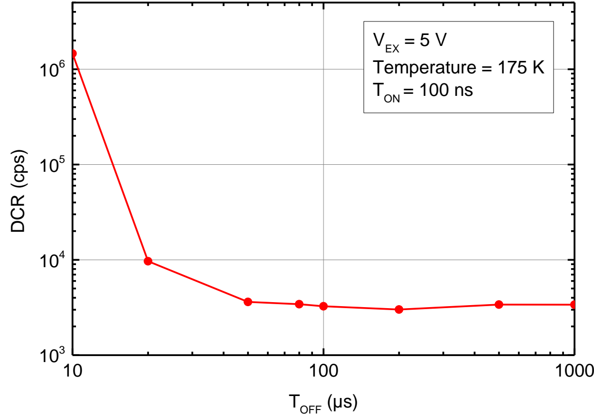

Fig. 8: Dark counts rate versus OFF time at 175 K for PoliMi SPAD sample 1: even at this low temperature, the DCR at T_{OFF} = 100 μs is comparable to that at much longer T_{OFF}, i.e. the so-called primary dark count rate.

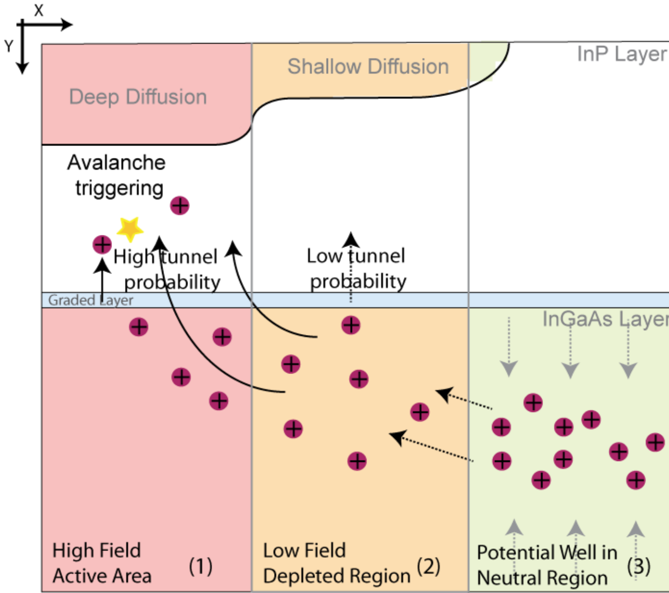

Fig. 9: Schematic representation of the charge persistence mechanism. Three regions are identified with high, low, and almost zero (neutral) electric field.

guaranteeing lower holes pile-up and, eventually, lower charge persistence.

IV. Modeling and Simulations

From the above-reported experimental characterization, we conceived a physical model for the charge persistence phenomenon.

In Fig. 9, the InGaAs layer is schematically divided into three regions: (1) a round one underneath the active area of the device, i.e. beneath the deep Zinc diffusion, where the electric field is very high; (2) a toroidal one (i.e. a hollow cylinder) acting as a transition, i.e. a depleted region extending from the deep Zn diffusion edge to a point at which the absorption layer is no more depleted; (3) an outer toroid, where the InGaAs is neutral, since electric field is very low.

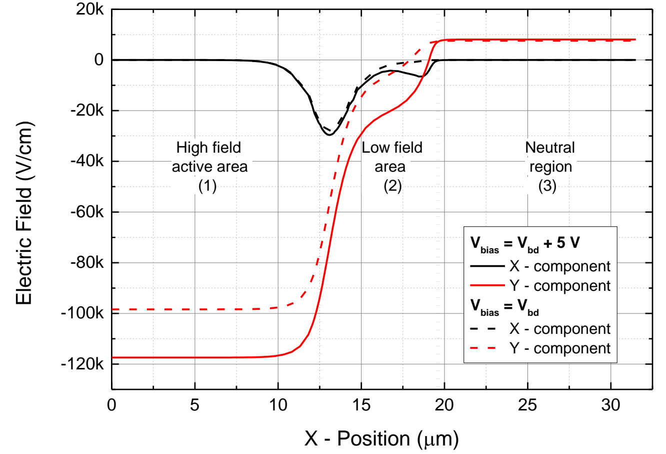

Fig. 10: Simulated horizontal (x) and vertical (y) electric field components at the InGaAs/InP heterointerface for a typical PoliMi SPAD.

From the simulations shown in Fig. 10, the vertical (Y direction) electric field component at the heterobarrier is maximum in region 1, decreases towards zero in region 2 and changes sign in region 3. The electric field of region 3 is due to the band bending that occurs at the isotype heterojunction because of the work function difference. Therefore, holes generated in the neutral region 3 cannot overcome the heterobarrier there, because of the repulsive electric field (see simulation in Fig. 10), but they can diffuse in the InGaAs layer eventually reaching region 2. Since the hole mean free path for bulk InGaAs is quite long (tens of μm as reported in literature [4][5]), region 2 can collect holes coming from a large volume of region 3. By following the procedure illustrated in [4], we measured the diffusion length. The experimental steady-state photocurrent is measured as a function of the distance of the laser spot from the active area (see Fig. 11). Neglecting surface recombination, the exponential decay derived in [4] holds for the photocurrent I(x):

$$I(x) = I(0) \cdot \exp(-x/L),$$

where x is the laser spot distance from the edge of the active area and L is the minority carrier diffusion length. Using an exponential fitting of the photocurrent decay, we extrapolated a hole diffusion length L longer than 70 μm at 235 K, in agreement with [5].

After diffusion from region 3 to region 2, the vertical field in region 2 drifts holes towards the upper heterointerface. However, some of those holes fail to cross the heterobarrier there, because of the low electric field that gives a low crossing probability. Since region 2 is depleted, those holes do not recombine, but they horizontally drift to region 1 with an average velocity of few μm/ns, due to the x electric field component (see simulation of Fig. 10).

Holes reaching the active area (region 1) before gate-ON are vertical drifted towards the InP multiplication region thanks to the high crossing probability, but they do not trigger avalanches. Instead, holes drifting into the active area during

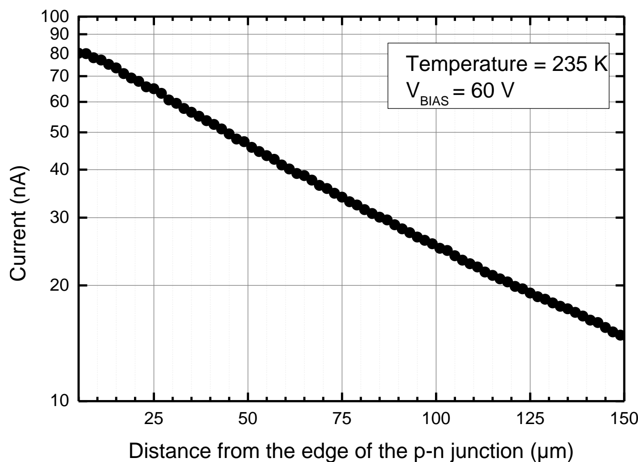

Fig. 11: Steady-state photocurrent as a function of the distance from the edge of the p-n junction.

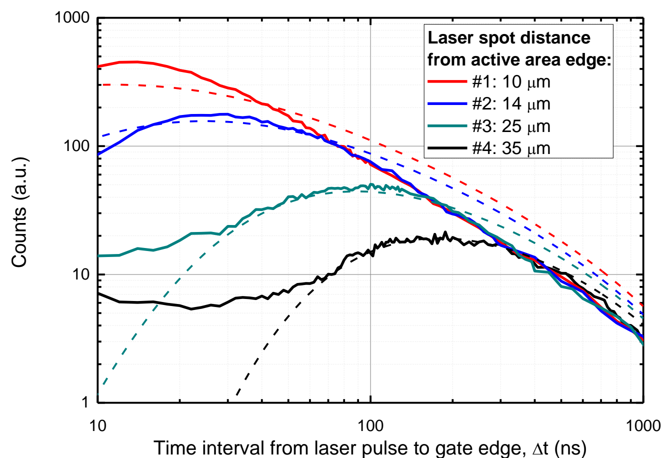

Fig. 12: Counts of the SPAD as a function of the time interval from laser pulse to gate edge, with the illumination spot at different distances from the edge of the active area. Measurement data are shown with continuous lines, simulation ones with dashed lines. Operating conditions: V_{EX} = 5 V, V_{UV} = 0.5 V, T_{ON} = 20 ns, T_{OFF} = 100 µs.

the gate-ON time can ignite spurious avalanches.

In order to confirm our model, we repeated the measurements reported in Fig. 3, but with the laser pulse focused in the device periphery with distances of 10, 14, 25 and 35 µm from the edge of the active area. As shown in Fig. 12 the laser spot position strongly affects the shape of the excess counts decay. In detail, for a given Δt, the higher the spot distance from the active area, the longer the delay of the peak in the count distribution from the gate opening, because of the finite velocity of the carriers entering the active area.

When the laser is focused at 10 µm from the edge of the active area, the persistence counts have a maximum after 16 ns. Instead, if the laser is focused 35 µm away, the maximum is at 150 ns, from which we can estimate a mean diffusion velocity of 180 nm/ns.

V. Conclusions

We presented an extended characterization of the charge persistence effect for InGaAs/InP SPADs. Specifically, the diffusion of holes in the neutral region of the InGaAs layer towards the active area can be a limiting factor for the performance of InGaAs/InP SPADs. Therefore, we proposed a complete physical model, based on the demonstration that holes generated in the periphery of the detector can anyway reach the active area and trigger false counts, thus introducing distortion and reducing the dynamic range in photon counting applications. We performed measurement down to 210 K and we estimated that there is a 3% probability that a photon absorbed 10 ns before the gate outside the active area triggers an avalanche. Additionally, the strong temperature dependence of this kind of noise limits the minimum operating temperature, potentially becoming the main noise contribution.

In order to reduce the charge persistence and its impact, the barrier crossing probability in region 2, where the avalanche triggering efficiency is very low, has to be increased by tailoring the electric fields and the heterobarrier. Generally speaking, possible solutions could be: i) to optimize the difference in depth between deep and shallow Zinc diffusions, while keeping almost the same active area uniformity, in order to increase the electric field in the peripheral region; ii) to tailor the doping in the charge layer and in the absorption layer in order to increase the electric field at the heterojunction, with the drawback of a possible increase in the dark count rate due to trap assisted tunneling; iii) to cover the peripheral region with a metal layer for preventing photon absorption outside the active area; iv) to introduce a contacted guard ring in order to sink the holes generated outside the active area.

References

[1] X. Jiang, M.A. Itzler, R. Ben-Michael, K. Slomkowski, “InGaAsP–InP Avalanche Photodiodes for Single Photon Detection,” IEEE Journal of Selected Topics in Quantum Electronics, vol 13, no 4, pp. 895 – 905, 2007.

[2] A. Tosi, F. Acerbi, M. Anti, F. Zappa, “InGaAs/InP single photon avalanche diode with reduced afterpulsing and sharp timing response with 30 ps tail,” IEEE J. Quantum Electron., vol. 48, no. 9, pp. 1227–1232, 2012.

[3] A. Tosi, N. Calandri, M. Sanzaro, and F. Acerbi, “Low-Noise, Low-Jitter, High Detection Efficiency InGaAs/InP Single-Photon Avalanche Diode,” IEEE J. Sel. Top. Quantum Electron., vol. 20, no. 6, pp. 1–6, 2014.

[4] R. Trommer and L. Hoffmann, “Large-hole diffusion length and lifetime in InGaAs/InP double-heterostructure photodiodes,” Electron. Lett., vol. 22, no. 7, p. 360, 1986.

[5] M. Gallant and a. Zemel, “Long minority hole diffusion length and evidence for bulk radiative recombination limited lifetime in InP/InGaAs/InP double heterostructures,” Appl. Phys. Lett., vol. 52, no. 20, pp. 1686–1688, 1988.

[6] Y. Matsushima et al., “High-speed-response InGaAs/InP heterostructure avalanche photodiode with InGaAs buffer layers,” Electron. Lett., vol. 18, no. 22, pp. 18–19, 2000.

[7] A. Zemel and M. Gallant, “Current-voltage characteristics of metalorganic chemical vapor deposition InP/InGaAs p-i-n photodiodes: The influence of finite dimensions and heterointerfaces,” J. Appl. Phys., vol. 64, no. 11, pp. 6552–6561, 1988.

[8] I. Bargigia, A. Tosi, A. Bahgat Shehata, A. Della Frera, A. Farina, A. Bassi, P. Taroni, A. Dalla Mora, F. Zappa, R. Cubeddu, and A. Pifferi, “Time-resolved diffuse optical spectroscopy up to 1700 nm by means of a time-gated InGaAs/InP single-photon avalanche diode.,” Appl. Spectrosc., vol. 66, no. 8, pp. 944–50, 2012.

[9] G. Boso, B. Korzh, T. Lunghi, B. Sanguinetti, and H. Zbinden, “Low noise InGaAs/InP single-photon detector for singlet oxygen detection,”

Proc. SPIE 9370, Quantum Sens. Nanophotonic Devices XII, vol. 9370, p. 93701S, 2015.

[10] M. A. Itzler, U. Krishnamachari, M. Entwistle, M. Owens, and K. Slomkowski, “Dark Count Statistics in Geiger-Mode Avalanche Photodiode Cameras for 3-D Imaging LADAR,” IEEE J. Sel. Top. Quantum Electron., vol. 20, no. 6, pp. 318–328, Nov. 2014.

[11] A. Dalla Mora, D. Contini, A. Pifferi, R. Cubeddu, A. Tosi, and F. Zappa, “Afterpulse-like noise limits dynamic range in time-gated applications of thin-junction silicon single-photon avalanche diode,” Appl. Phys. Lett., vol. 100, pp. 241111–241114, 2012.

[12] J. Zhang, R. Thew, J.-D. D. Gautier, N. Gisin, and H. Zbinden, “Comprehensive Characterization of InGaAs–InP Avalanche Photodiodes at 1550 nm With an Active Quenching ASIC,” IEEE J. Quantum Electron., vol. 45, no. 7, pp. 792–799, 2009.

[13] P. Eraerds, M. Legré, J. Zhang, H. Zbinden, N. Gisin, “Photon counting OTDR: advantages and limitations”, Journal of lightwave technologies, Vol. 28, No. 6, March 2010.

Niccolò Calandri was born in Como, Italy, in 1989. He received the B.Sc. degree in Biomedical Engineering in 2011 and the M.Sc degree in Electronic Engineering in 2013 at Politecnico di Milano, summa cum laude. Since November 2013 he is a Ph.D. candidate in Electronic Engineering at Politecnico di Milano. Curretly, he worked on design and characterization of III-V single-photon avalanche diodes (SPADs) and superconducting nanowire single photon detector (SNSPD) with innovative structures.

Mirko Sanzaro was born in Avola, Italy, in 1988. He obtained the Bachelor Degree in Electronic Engineering in 2010, and the M.Sc. Degree (summa cum laude) in Electronic Engineering in October 2013, both at Politecnico di Milano. Since November 2013 he is a Ph.D. candidate in Electronic Engineering at Politecnico di Milano. His current research activity aim at the design, development and characterization of near-infrared (NIR) single-photon avalanche diodes (SPADs).

Alberto Tosi (M’07) was born in Borgomanero, Italy, in 1975. He received the master’s degree in electronics engineering and the Ph.D. degree in information technology engineering from the Politecnico di Milano, Milan, Italy, in 2001 and 2005, respectively. He was an Assistant Professor from 2006 to 2014. He has been an Associate Professor of Electronics with the Politecnico di Milano since 2014. In 2004, he was a Student with the IBM T. J. Watson Research Center, Yorktown Heights, NY, working on optical testing of CMOS circuits. He currently works on silicon and InGaAs/InP single-photon avalanche diodes (SPADs). His research activity includes arrays of silicon SPADs for 2-D and 3-D applications and time-correlated single-photon counting electronics.

Franco Zappa Zappa (M’00–SM’07) was born in Milan, Italy, in 1965. He received the Master degree in electronic engineering and the Ph.D. degree in electronic and communication engineering from Politecnico di Milano, Milan, Italy, in 1989 and 1993, respectively. Since 2011 he is Full Professor of electronic systems with the Department of Electronics, Information Science, and Bioengineering at Politecnico di Milano. He pioneered and deployed novel single-photon avalanche diodes (SPAD) structures in both Silicon and InGaAs/InP semiconductors, in both standard CMOS and custom processing. In 1994, he presented and patented the design of the first monolithic active quenching circuit electronics for single-photon detection. He has co-authored more than over 120 papers published in international peer-reviewed journals and in proceedings of international conferences, and five text books on the fundamentals of electronics and electronic systems. His current research interests include design and development of microelectronic circuits and CMOS SPAD imagers for the visible and near-infrared wavelength range, high-sensitivity luminescence measurements, 2D image acquisitions, and 3D depth ranging. He co-founded Micro Photon Devices, a leading company in the worldwide market of photon counting instrumentation.